Development of Numerical Model of KSTAR PF Conductor and Magnet for the Analyses of AC Loss on the Results of KSTAR PF Magnet Test Run

Dong Keun Oh, Hyun Jung Lee, Sang-Hee Hahn, Yeong-Kook Oh, and Keeman Kim

***Abstract*—To analyse the experimental results of PF magnet during the commissioning test of KSTAR, a numerical model of the PF1 magnet and its CICC was developed for the evaluation of Joule heat from the AC loss due to the time varying field profile along the conductor during ramping-up or down taking into account the ferromagnetic effect of Incoloy 908 jacket. The calculation routines was carefully updated to make a proper estimation of the AC loss and applied to the estimation of AC loss parameters of the CICC of the KSTAR PF magnet.**

***Index Terms*—CICC AC loss, Incoloy 908, KSTAR.**

I. Introduction

DURING the commissioning test of the Korea Super-conducting Tokamak Advanced Research (KSTAR) device, various charging tests were carried out as a first test of superconducting magnet after the assembly. Among those tests, calorimetric AC-loss tests were carried out for the PF1 magnet [1], which is the most central part of CS coil magnet in KSTAR system, not only to monitor the basic safety of the newly fabricated magnet, but also to evaluate AC-loss parameters which are known to be changed after assembly in some cases [2]. During the commissioning test, the AC-loss was to be estimated as precisely as possible, because the AC-loss is the key parameter to determine the power dissipation in the operation of superconducting tokamak, which requires cooling power to maintain the magnet system in the safe operating condition.

The PF1 charging experiment was planned to apply two types of waveform of the current—one is trapezoidal ramping up & down and the other is sinusoidal current loading with a DC bias—for the commissioning test. Among those test runs, various ramping rates (0.5 kA/s $\sim$ 2 kA/s) were tried for the trapezoidal ramping test to estimate the constant of coupling loss $n\tau$. The power dissipation was estimated from the temporal evolution data of thermo-hydraulic variables $(T, P, dm/dt)$ which measured at the appropriate positions on thee cooling channel.

Manuscript received October 20, 2009. First published April 08, 2010; current version published May 28, 2010. This work was supported by the Korean Ministry of Science and Technology of Republic of Korea under the Contract of ITER Korea Project and KSTAR Project.

The authors are with the National Fusion Research Center, Daejeon, Republic of Korea (e-mail: spinhalf@nfri.re.kr).

Color versions of one or more of the figures in this paper are available online at http://ieeexplore.ieee.org.

Digital Object Identifier 10.1109/TASC.2010.2044163

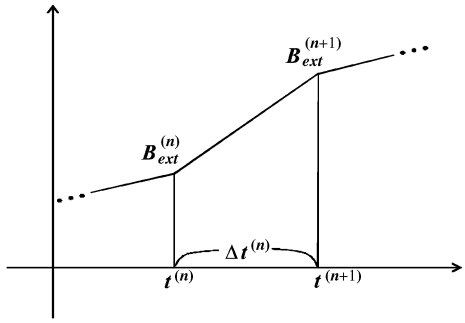

Fig. 1. Piecewise linear interpolation of magnetic field.

At the beginning, we decided to develop a numerical model to interpret the result of AC loss test of PF1 attempting to apply a similar technique to analyses of superconducting magnet in a certain case which requires relatively accurate model taking into account the nonlinear effect of the ferromagnetic jacket material (Incoly 908) of the CICC in the KSTAR PF magnet. The ferromagnetic effect was supposed to be assessed at least one time on the magnetic field profile and its influence on the AC-loss calculation, even if it will be turned out to be negligible.

II. Numerical Model

A. Piecewise Linear Approximation of Magnetic Field

To describe an arbitrary waveform of transient magnetic field, a piecewise linear interpolation can be applied as presented as in Fig. 1. For the calculation of AC-loss, the joule heat will be evaluated for every time step assuming that the applied magnetic field is a linear function of time which is continuous between the steps. Governing equations for the AC-loss are to be solved for the interval between the steps being correlated to each other by the proper causal relation.

At each time domain $(t^{(n)}, t^{(n+1)})$, the Joule heat from the AC-loss during the linear ramping, i.e. $\Delta Q^{(n)}$, can be expressed as

$$\Delta Q^{(n)} = \sum_{\substack{k=Hysteresis,\\ Coupling\ etc.}} \overline{M}_k^{(n)} \Delta B_k^{(n)} A_k \quad (\mathrm{J/m}) \qquad (1)$$

For the nth time interval $\Delta t^{(n)}$, the Joule heat per length can be formulated by the sum of the product of the area A of the heat generation and the magnetic loss per volume which can be formulated as $M\Delta B$ for each component of AC loss i.e. the

hysteresis loss the coupling loss of the strand and the cable and so on.

At a certain moment in the time domain, the applied magnetic field can be described as

$$\begin{aligned} \boldsymbol{B_{ext}}(t) &= \boldsymbol{B_{ext}^{(n)}} + \boldsymbol{b_{ext}^{(n)}}\left(\boldsymbol{t} - \boldsymbol{t^{(n)}}\right) \\ \boldsymbol{b_{ext}^{(n)}} &= \left(\boldsymbol{B_{ext}^{(n+1)}} - \boldsymbol{B_{ext}^{(n)}}\right)/\Delta \boldsymbol{t^{(n)}} \end{aligned} \tag{2}$$

B. Hysteresis Loss and Coupling Loss

Hysteresis loss of superconducting filaments is caused by changing persistent current with respect to the field variation, which appears hysteretic behavior of magnetization depending on the penetration of external field from the outside of the superconducting filament.

For the piecewise calculation, hysteresis loss at a certain time interval will be given to be

$$\Delta \boldsymbol{Q_{Hyst}^{(n)}} = \overline{\boldsymbol{M}}^{\boldsymbol{(n)}} \Delta \boldsymbol{B^{(n)}} \boldsymbol{A_{non-Cu}} \tag{3}$$

, where the average of magnetization and the difference of magnetic field are

$$\begin{aligned} \overline{\boldsymbol{M}}^{\boldsymbol{(n)}} &= \frac{1}{2}\left(\boldsymbol{M^{(n+1)}} + \boldsymbol{M^{(n)}}\right) \\ \Delta \boldsymbol{B^{(n)}} &= \boldsymbol{B^{(n+1)}} - \boldsymbol{B^{(n)}} \end{aligned} \tag{4}$$

And, the magnetization can be described as [3]

$$\boldsymbol{M} = \begin{cases} \frac{2}{3\pi}\boldsymbol{j_c D_{eff}}\left(1 + \left(\frac{\boldsymbol{I_{tr}}}{\boldsymbol{I_c}}\right)^2\right) & (\boldsymbol{B} > \boldsymbol{B_p}) \\ \frac{\boldsymbol{B}^2}{6\mu_0 \boldsymbol{B_p}}\left(1 - \frac{\boldsymbol{B}}{4\boldsymbol{B_p}}\right) & (\boldsymbol{B} < \boldsymbol{B_p}) \end{cases} \tag{5}$$

, where B_p is $\mu_0 j_c D_{eff}/\pi$, D_{eff} is the effect filament diameter in the superconducting strands, j_c and I_c are the critical current density and the critical current respectively and I_{tr} is the transport current.

Paying attention to the hysteresis loss during the linear ramping, the resultant formula indicates that the Joule heat during the piecewise ramping is nothing to do with the length of time interval, but only depends on the differential amplitude of magnetic field.

On the other hand, there is the coupling loss which is originated from the inductive loops whose resistive couplings are distributed among the strands in cable or within the strand. Thus, the delay from the effective time constant of inductive loops τ should be taken into account for the governing equation [4]

$$\Delta \boldsymbol{Q_{Cpl}^{(n)}} = \frac{\boldsymbol{n\tau}}{\boldsymbol{\mu_0}}\left(\dot{\boldsymbol{B}}_{\mathrm{int}}^{\boldsymbol{(n)}}\right)^2 \Delta \boldsymbol{t^{(n)}} \tag{6}$$

$$\dot{\boldsymbol{B}}_{\mathrm{int}} + \frac{\boldsymbol{B}_{\mathrm{int}}}{\boldsymbol{\tau}} = \frac{\boldsymbol{B_{ext}}}{\boldsymbol{\tau}} \tag{7}$$

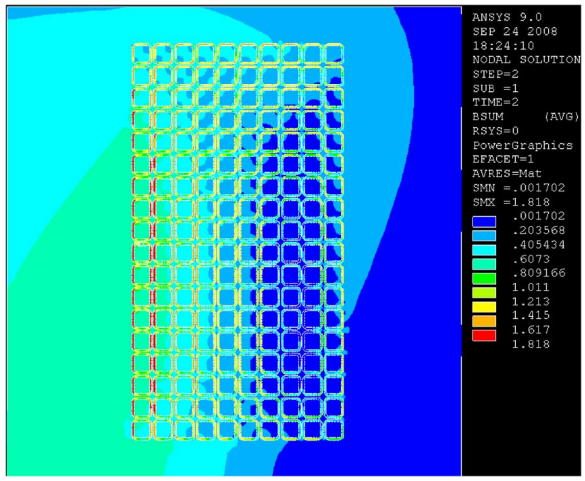

Fig. 2. A contour plot of magnetic field with PF1 magnet at 2 kA: counted from bottom layer, 3rd, 4th, 5th, and 6th layers belong to the cool channel #5 whose temperature was analysed for the AC loss calculation in this article.

If (7) is solved assuming the external field as (2), $\dot{B}_{\mathrm{int}}^{(n)}$ can be express as following

$$\dot{\boldsymbol{B}}_{\mathrm{int}}^{\boldsymbol{(n)}} = \boldsymbol{b_{ext}^{(n)}}\left(1 - \boldsymbol{e}^{-\Delta \boldsymbol{t^{(n)}}/\boldsymbol{\tau}}\right) + \boldsymbol{b^{(n)}}\boldsymbol{e}^{-\Delta \boldsymbol{t^{(n)}}/\boldsymbol{\tau}} \tag{8}$$

where

$$\begin{cases} \boldsymbol{b^{(n)}} = \boldsymbol{b_{ext}^{(n-1)}}\left(1 - \boldsymbol{e}^{-\Delta \boldsymbol{t^{(n-1)}}/\boldsymbol{\tau}}\right) + \boldsymbol{b^{(n-1)}}\boldsymbol{e}^{-\Delta \boldsymbol{t^{(n-1)}}/\boldsymbol{\tau}} \\ \boldsymbol{b^{(1)}} = 0 \end{cases} \tag{9}$$

While some conventional formulae have been applied to the cases of the linear ramping and the sinusoidal waveform [5], [6], the set of recurrence relations of (8) and (9) could provide us a more general expression of the coupling loss based on the piecewise interpolation of the arbitrary field.

C. 2D FE Model for Magnetic Field

A numerical model of PF1 was developed for the commercial FEM analysis software (ANSYS-EM) to evaluate an accurate 2D magnetic field profile (Fig. 2) during the ramping up and down of the PF1 and PF2 which is located at the center of the CS (central solenoid) winding packs in KSTAR. Based on the precise geometry of the cross-section, the 2D mesh of the FE model was developed for the static case of the calculation of the perpendicular component of magnetic vector potential to obtain the magnetic field which is only parallel to the plane of 2D model.

The B-H curve at 4.5 K in Fig. 3 of ferromagnetic Incoloy 908 was assigned in the FE mode as a non-linear material property of ANSYS model, which was the magnetic property for the jacket material of CICC of KSTAR device after the heat treatment, which has been measured using a SQUID magnetometer domestically.

Individual time derivatives of the magnetic field at the center of each CICC in the 3rd layer were presented in Fig. 4. Time

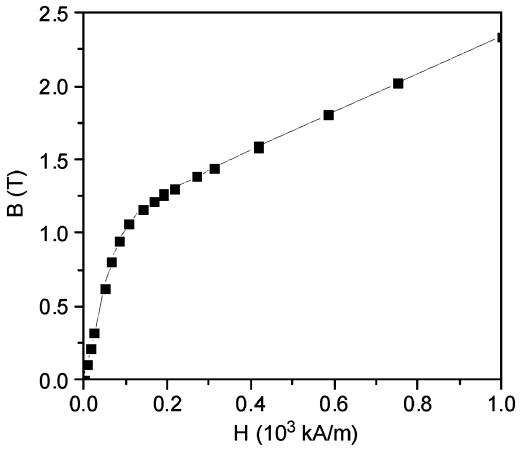

Fig. 3. Magnetic field versus external field intensity of Incoloy 908 at 4.5 K.

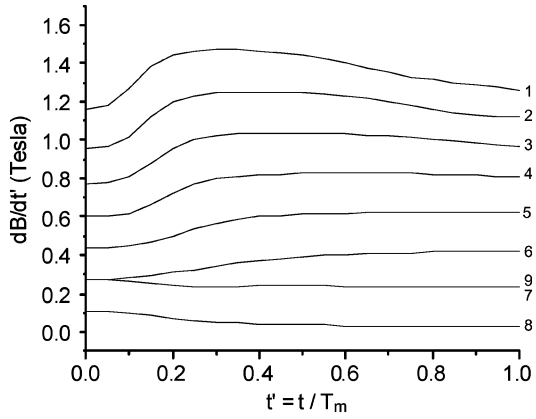

Fig. 4. Individual time derivatives of magnetic field with normalized time t' at the 3rd layers from bottom of PF1. Turn indexes were counted from the inner most CICC. Maximum current is 4 kA, Ramping time T_m was2, 4 or 8 second.

is normalized by the duration of ramping up to 4 kA for convenience. To cope with such a normalization, (8) and (9) was modified to be $\Delta \boldsymbol{t}^{(\boldsymbol{n})} \rightarrow \Delta \boldsymbol{t}'^{(\boldsymbol{n})}$ and $\boldsymbol{\tau} \rightarrow \boldsymbol{\tau}'$, where $\Delta \boldsymbol{t}'^{(\boldsymbol{n})} = \Delta \boldsymbol{t}^{(\boldsymbol{n})}/\boldsymbol{T_m}$ and $\boldsymbol{\tau}' = \boldsymbol{\tau}/\boldsymbol{T_m}$.

III. Discussion

For the evaluation of slopes of internal field with the result from FE model, we applied the developed formulae of (8) and (9). Assessing the effect of ferromagnetic jacket material, discussion was made about the effect of delay due to the time constant of inductive couplings, and we presented the analysis of the PF1 calorimetric AC loss experiment with various ramping rates of trapezoidal current load.

A. Effect of Time Constant

We demonstrated the effect of coupling time constant causing the delay in the evolution of internal magnetic field. Using the normalized time scale, the evaluated internal field slopes for the 1st graph in Fig. 4 are displayed with respect to relative quantity of time constant $\boldsymbol{\tau}'$ in Fig. 5.

The Fig. 5 shows that only if the order of magnitude of the duration time is twice bigger than the time constant of the inductive delay, we can neglect the effect of inductive delay of

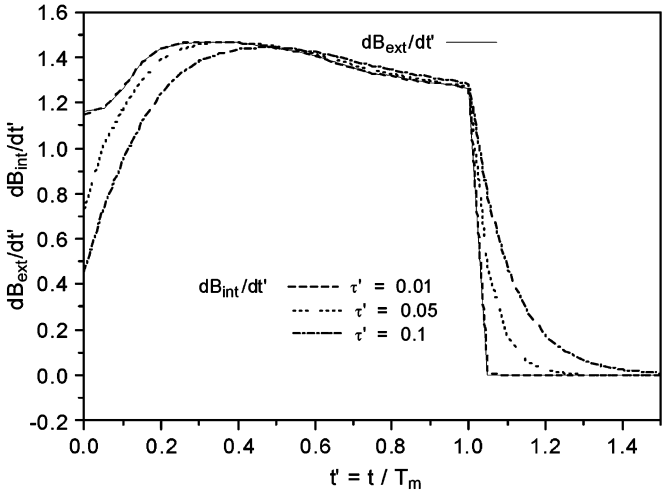

Fig. 5. Evaluation of internal field: Eqs. (8) and (9) was applied to the time derivative of external field at the 1st turn (Figs. 2 and 4) assuming several values of normalized time constant.

coupling loss in that case. Conventionally, the time constant τ itself has not been taken into account the analysis of the AC loss of superconductor; because the magnitude of the coupling loss is directly proportional to $n\tau$ in which the shape factor of the coupling loops n is reflected. According to the result, the time constant τ could assess the accuracy of the calculation when we employed of the applied magnetic field instead of the internal field. However, in the case of KSTAR PF test run, such an approximation looks reasonable, if we compared the assessed $n\tau$ value, which is shown in the next section, with the duration times of linear ramping.

B. Analysis of PF1 Test Run of Trapezoidal Ramping

As we mentioned above, PF1 test was carried out with various duration times of ramping [1]. Trapezoidal pulses were applied in the test run is presented in Fig. 6.

The AC loss was analysed through the calorimetric measurement data from the channel #5 whose response was the most suitable to be investigated because of its larger response in temperature than any other one. In consequence of the calorimetric analysis, the total Joule heat data were obtained with respect to the ramping rates. The errors of each calorimetric measurement were small enough to determine the coupling loss constant to be precise in the order of millisecond.

After the evaluation of applied field from the FE model in the Section II, the normalized time derivative of magnetic field of each CICC were employed to estimate the AC loss parameters of PF1 conductor using the next formula.

$$\begin{aligned}\Delta \boldsymbol{q}[\boldsymbol{J}] &= 2\frac{\boldsymbol{n\tau}}{\boldsymbol{\mu_0 T_m}} \sum_{\boldsymbol{i}=1}^{16} 2\pi \boldsymbol{R_i} \int_0^1 \left(\left[\frac{\boldsymbol{dB}_{\rm int}}{\boldsymbol{dt'}} \right]_{\boldsymbol{i}} \right)^2 \boldsymbol{dt'} \boldsymbol{A_{Cable}} \\ &\quad + \Delta \boldsymbol{q_{hyst}} \\ &= 2\frac{\boldsymbol{n\tau}}{\boldsymbol{\mu_0 T_m}} \boldsymbol{L_{total}} \overline{\int_0^1 \left(\frac{\boldsymbol{dB}_{\rm int}}{\boldsymbol{dt'}} \right)^2 \boldsymbol{dt'}} \boldsymbol{A_{Cable}} \\ &\quad + \Delta \boldsymbol{q_{hyst}} \end{aligned} \tag{10}$$

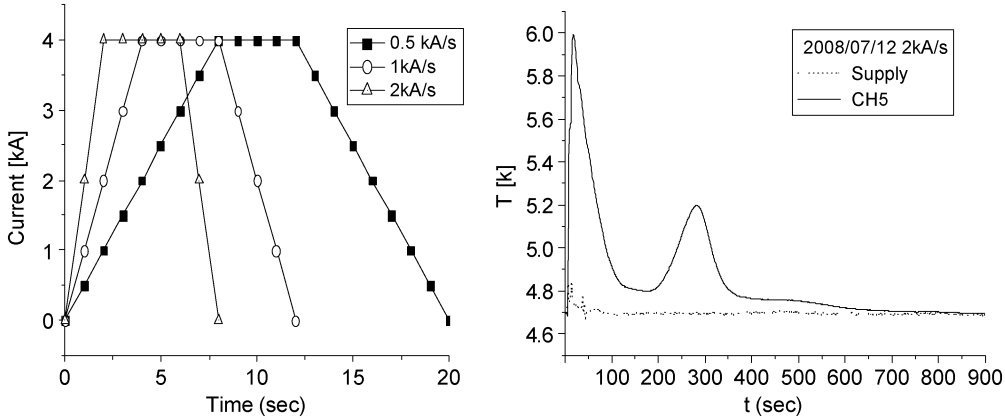

Fig. 6. The trapezoidal ramping pulse shapes employed to the test (left), Temperature variation of channel #5 whose response was the biggest than the other cooling channels of PF1 due to the largest average ramp rate of magnetic field in the case of 2 kA/s (right).

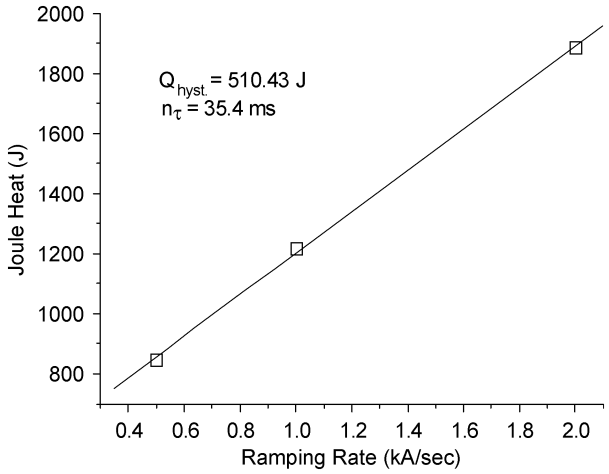

Fig. 7. Ramping rate versus calorimetric measurement: Using the slope of this plot and numerical evaluation of the derivatives of magnetic field, AC loss parameters were successfully estimated.

During the integral in (10), the time constant τ was assumed to be small enough in comparison with the ramping times. Least square fitting was employed to find two unknowns in (10), and the result of the analysis is present in Fig. 7.

In consequence, $n\tau$ is assessed as 35 ms and total amount of hysteresis loss during the trapezoidal ramping up to 4 kA was estimated to be 510.4 J which corresponds to $\sim$180 mJ/cc. Thus, the specification of the hysteresis loss of Nb_3Sn strands, which is below 250 mJ/cc for $\pm$3 T at 4.2 K [7], is consistent with the estimation of the total hysteresis loss of the channel #5 of the PF1 magnet. The coupling constant is about twice bigger than the previous estimation, which was obtained from the experiment of the KSTAR CSMC test [7]. The detail analysis compared with the previous test run is presented in elsewhere [8].

IV. Conclusion

Based on the approach of piecewise linear interpolation of magnetic field, an AC loss evaluation were introduced. It was applied to the time derivative of magnetic field of KSTAR PF1 during the trapezoidal current ramping, which was calculated through the developed FE model taking into account the ferromagnetic effect of Incoloy 908 jacket. After demonstration of the delay of internal field with respect the relative time constant of effect RL loop of coupling loss, PF1 commissioning test results were analysed employing developed numerical model to assess the AC loss parameters of KSAR PF1 magnet.

References

[1] Y. K. Oh and W. C. Kim *et al.*, "Commissioning and initial operation of KSTAR superconducting tokamak," *Fusion Engineering and Design*, vol. 84, pp. 344–350, 2009.

[2] T. Hamajima *et al.*, "A mechanism causing as additional AC loss in a large CICC coil," *IEEE Trans. Applied Superconductivity*, vol. 11, pp. 1860–1863, 2001.

[3] Q. Wang, C. S. Yoon, J. He, W. Chung, and K. Kim, "Operating temperature margin and heat load in PF superconducting coils of KSTAR," *IEEE Trans. Appl. Supercond*, vol. 12, pp. 648–652, 2002.

[4] L. Bottura and F. Rosso, "AC loss calculation algorithm," Cryosoft Internal Note CRYO/97/001, Aug. 2006.

[5] C. Y. Gung, M. Takayasu, and J. V. Minervini, "Experimental estimation of energy dissipation in ITER central solenoid superconductor," in *Proc. 15th IEEE/NPSS Symp.*, New York, 1994, pp. 692–695.

[6] A. Nijhuis, N. H. W. Noordman, and H. H. J. ten Kate, "Electromagnetic and mechanical characterization of ITER CS-MC conductors affected by transverse cyclic loading, part 1 L coupling current loss," *IEEE Trans. Appl. Supercond*, vol. 9, no. 2, pp. 1069–1072, 1999.

[7] S. Lee, Y. Chu, W. H. Chung, S. J. Lee, S. M. Choi, S. H. Park, H. Yonekawa, S. H. Baek, J. S. Kim, K. W. Cho, K. R. Park, B. S. Lim, Y. K. Oh, K. Kim, J. S. Bak, and G. S. Lee, "AC loss characteristics of the KSTAR CSMC estimated by pulse test," *IEEE Trans. Appl. Supercond*, vol. 16, no. 2, pp. 771–774, 2006.

[8] H. J. Lee, D. K. Oh, Y. Chu, Y. M. Park, H. T. Park, J. H. Choi, S. H. Hahn, K. R. Park, Y. K. Oh, and H. L. Yang, "The AC loss measurement of the KSTAR PF1 coils during the first commissioning," presented at the MT-21 Conference, Hefei, China, Oct. 21, 2009, (submitted to *IEEE Trans. Appl. Supercond.*).